

PAPER • OPEN ACCESS

## Buckling of thin walled composite cylindrical shell filled with solid propellant

To cite this article: A P Dash *et al* 2017 *IOP Conf. Ser.: Mater. Sci. Eng.* **270** 012022

View the [article online](#) for updates and enhancements.

### Related content

- [Collapse of composite tubes under uniform external hydrostatic pressure](#)  
P T Smith, C T F Ross and A P F Little
- [The axial crushes behaviour on foam-filled round Jute/Polyester composite tubes](#)  
A Othman and A E Ismail
- [STARS HAVING SHELL SPECTRA](#)  
Paul W. Merrill

# Buckling of thin walled composite cylindrical shell filled with solid propellant

A P Dash<sup>1</sup>, R Velmurugan<sup>1,\*</sup> and M S R Prasad<sup>2</sup>

<sup>1</sup>Department of Aerospace Engineering, Indian Institute of Technology, Madras, Chennai, India

<sup>2</sup>Defence Research and Development Organization, India

\* ramanv@iitm.ac.in

**Abstract.** This paper investigates the buckling of thin walled composite cylindrical tubes that are partially filled with solid propellant equivalent elastic filler. Experimental investigation is conducted on thin composite tubes made out of S2-glass epoxy, which is made by using filament winding technique. The composite tubes are filled with elastic filler having similar mechanical properties as that of a typical solid propellant used in rocket motors. The tubes are tested for their buckling strength against the external pressure in the presence of the filler. Experimental data confirms the enhancement of external pressure carrying capacity of the composite tubes by up to three times as that of empty tubes for a volumetric loading fraction (VLF) of 0.9. Furthermore, the finite element based geometric nonlinearity analysis predicts the buckling behaviour of the partially filled composite tubes close to the experimental results.

## 1. Introduction

Composites have established itself as a strong alternative to metals in the field of rocketry. Composite rocket motor casings (CRMC) have become more popular in rocketry due to its inherent advantage in terms of specific strength. CRMC are filled with solid propellant at few different volumetric loading to meet the various mission requirements. In order to reduce the size of the rocket, volumetric loadings of 90% and above have become common practice in many cases. Solid propellant is a polymeric material that is poured into CRMC and cured at a specified temperature environment. This polymer is similar to a soft elastomeric material with regards to its mechanical behavior. At the time of structural design of the CRMC, one considers all possible load cases that the rocket undergoes throughout its mission. There are occasions when the rocket motor casings experience external pressure loading, which gives rise to a critical load case for which one has to design CRMC for buckling.

It has been a general practice to design CRMC alone to withstand buckling loads and the presence of solid propellant inside it is ignored. In this process, design of CRMC ends up with a conservative estimate. Efficient use of filament wound fiber reinforced CRMC requires a better knowledge of the structural response of the composite structure in the presence of solid propellant. Buckling behavior of thin shells with inner soft elastic filler, both with axial and external pressure loading, was investigated by many early researchers [1-4]. The closed form analytical approach to handle such cases has been discussed for isotropic cylindrical shells. The shell supported by an elastic foundation is the closest approach used by the authors to replicate the behavior of the shells in the presence of solid propellant. Karam and Gibson (1995) have reported experimental results of cylindrical silicon rubber shells with



and without complaint core under uniaxial load [5]. In their study, the thickness to radius ratio ( $t/r$ ) of shells were varied from 0.02 – 0.23. The thickness variation of the shells for the test was indicated to be of the order of 5% of nominal thickness and the elastic modulus ratio of the shell to core ( $E_s/E_c$ ) was of the order of 100. An increase of axial load carrying capacity of filled shells to an extent of 10 times with respect to empty tube has been reported in this study. Furthermore, Li (1998) has reported improvement of stability based on the results of finite element based theoretical investigation on metal and composite shells in the presence of elastic fillers [6]. In this study, composite shell was modeled using Sander's non-linear shell theory and filler propellant was modeled as Winkler-type foundation. This study reports extensively on the effect of initial geometric imperfections. A drop in buckling load carrying capacity to the tune of 11% has been indicated for isotropic shell with 1-20% of thickness imperfection. However, the effect of geometric imperfection was reported to be negligible in the case of the composite cylindrical shells.

It is a well-known fact that the buckling behavior of cylindrical structures is very much influenced by initial imperfections. Tsouvalis et al (2003) have studied the effect of geometric imperfections on buckling behavior of laminated composite cylindrical shells under external hydrostatic pressure [7]. In the study, both experimental and theoretical results are reported on carbon epoxy composite cylinders. The research concluded that it is essential to have a non-linear analysis to capture the behavior and it is enough to model the cylinder as a perfect mid-surface with average thickness that gives a knockdown factor of 0.6 to 0.7 on the buckling load in comparison to a perfect cylinder. This present study focuses on evaluating the effect of the presence of solid propellant (soft elastic filler) with various volumetric loading in a composite shell. The enhancement in the buckling load carrying capacity of the CRMC under external pressure loading at various volumetric loading has been experimentally investigated for quantification. Finite element based theoretical estimates are also presented for comparative purposes.

## 2. Composite Tubes

Depending upon the application, sizes of CRMC vary in their geometric parameters. In the present day rocketry, many of the CRMC sizes fall in the bracket of  $L/D$  between 1 to 5 and  $r/t$  between 50 to 150, where  $L$ ,  $D$ ,  $r$  and  $t$  are length, diameter, radius and thickness of the casing, respectively. The emphasis of this study is on behavior of thin walled composite tubes that are partially filled with solid propellant equivalent material. The cylindrical shells with  $L/D = 3$  and  $r/t = 100$  are chosen in the investigation, which is a fair representation of the class of CRMC in practical use. Based on the application, various types of composite material such as carbon-epoxy, glass-epoxy and Kevlar-epoxy have been used in the manufacturing of CRMC. In this study, glass epoxy is chosen as the material for the tubes. Figure 1 shows basic dimensions of the finished composite tubes. The selected tubes have an internal nominal diameter of 150mm and thickness of 2mm.

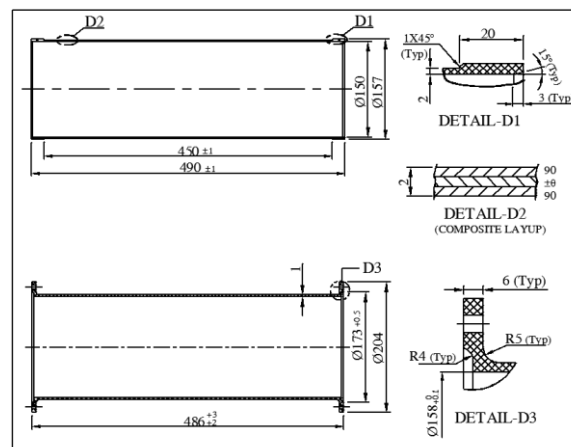


Figure 1: Dimensional details of composite tube and rubber bladder

S2-glass based tow pregs with epoxy resin has been chosen for the fabrication of composite tubes using filament winding technique. Figure 2 shows the steel mandrel on which CNC winding program is used to ensure a good quality product with acceptable repeatability in winding while Figure 3 shows the glass-epoxy tubes under winding. Infrared lamps are employed to ensure the proper resin softening during winding of tubes using tow pregs.



Figure 2: Steel mandrel with POP end domes ready for winding



Figure 3: Glass epoxy tube under winding using S2 glass tow prep

The nominal winding thickness of 2mm was achieved with individual layer thickness of 0.5mm. On the components, fibre volume fraction ( $V_f$ ) of 0.6 and density of 2.09 g/CC were obtained. After the winding and extraction of the composite tubes, they were inspected using ultrasonic technique to ensure there was no delamination of layers or any other damage to the tubes during processing. Two different winding patterns were chosen to make two types of tubes. They were designated as ‘Series-1’ with  $90^\circ$ ,  $\pm 45^\circ$ ,  $90^\circ$  winding and ‘Series -2’ with  $90^\circ$ ,  $\pm 30^\circ$ ,  $90^\circ$  winding pattern. Eighteen tubes from each of the series were fabricated for conducting experimental research. It is a well known fact that buckling load is a strong function of the initial geometry imperfection of the structure. All of these 36 tubes prepared for the experiments were dimensionally inspected to check for any geometric variation in diameters. Based on this measurement, initial radial geometric imperfection of 0.1mm was noticed on the tubes, which is 5% of the nominal thickness. This data was further utilized for finite element analysis later. Prior to the manufacturing of the tubes, the flat laminate level testing was conducted on S2 glass epoxy tow prep material. The achieved composite material properties are reported in Table 1. During the characterization of the laminates, suitable strain gauges were utilized for the determination of the Young’s modulus and Poisson ratio. In case of the Young’s modulus, single axis gauge was used while for the Poissons ratio, a  $90^\circ$  rosette was employed.

Table 1: Laminate level engineering properties of S2-glass towpreg

Sl. No.	Property	ASTM standard used for testing	Average Value
1	Longitudinal tensile strength	D3039	1648 MPa
2	Longitudinal tensile modulus	D3039	68 GPa
3	Major poisson ratio ( $\nu_{12}$ )	D3039	0.26
4	Transverse tensile strength	D3039	20 MPa
5	Transverse tensile modulus	D3039	21 MPa
6	Longitudinal compressive strength	D3410	969 MPa
7	Transverse compressive strength	D3410	124 MPa
8	Inplane shear strength	D3518	40 MPa
9	Inplane shear modulus	D3518	5 GPa
10	Density	D792	2.09 g/cc
11	Glass transition temp	E1356	184°C

The finished composite tubes were then internally lined with standard ROCASIN rubber of 0.5mm radial thickness and cured. This rubber lining is vital to ensure a good bonding between the composite tube and solid propellant fill. The rubber-lined tubes were filled with inert solid propellant filler that has equivalent mechanical properties as that of standard HTPB based solid rocket motor propellant composition with 18% Aluminum. Flat samples of the inert propellant were tested to determine their mechanical properties using ASTM standard D638. The set up used for testing the samples and the test specimens are shown in Figure 4. A typical force–extension curve obtained from this uni-axial testing of the above inert propellant material is presented in Figure 5. Since use of strain gauge is not possible for propellant samples, extensometer is utilized to record the extension history. Data of this curve is utilized to derive the Mooney Rivlin constants, which are applied in finite element analysis. The filling of composite tubes was done for five different volumetric loading fractions (VLF), which is defined as the ratio of volume of propellant to the inner volume of the empty tube. Empty and filled composite tube samples prepared for testing are depicted in Figure 6.



Figure 4: Inert propellant sample under uni-axial testing as per ASTM D638

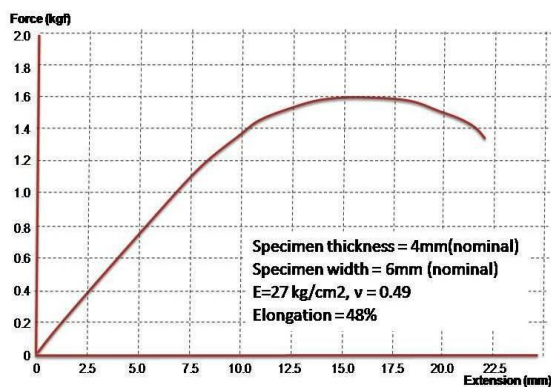


Figure 5: Experimental stress-strain curve of filler propellant material

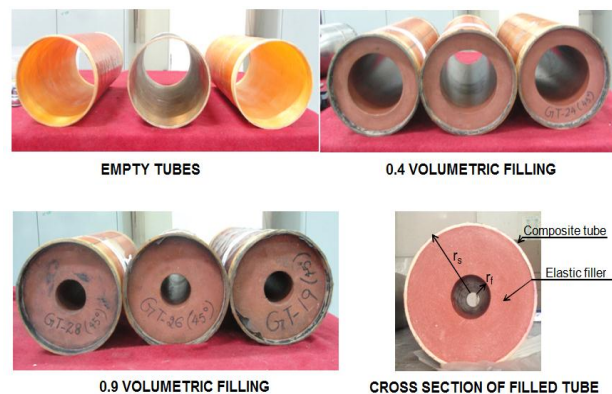


Figure 6: Typical photographs of empty and filled composite tubes

### 3. Experimental Test Setup

Since this investigation focuses on buckling of composite tubes under external pressure environment, a suitable tailor made test setup is realized to conduct these tests. Figure 7 presents the external pressure buckling setup. In short, a pressure chamber was fabricated out of structural steel with two end plates. Provision was made to support the shell under testing at either ends. The end conditions ensure that there is no translation and rotation of the shells at the point of support. The propellant filled composite tubes are assembled into the pressure chamber with two end plates supporting either end of the tube. The filament wound composite tubes are quite porous in nature and they need a mechanism to stop the entry of water through the thickness of the filament wound tubes. This has been achieved by sliding a thin

neoprene-based rubber bladder of 1mm thickness over the tube with the suitable dimension. To summarize, Figure 8 presents the photographs of the shell assembly at different stages.

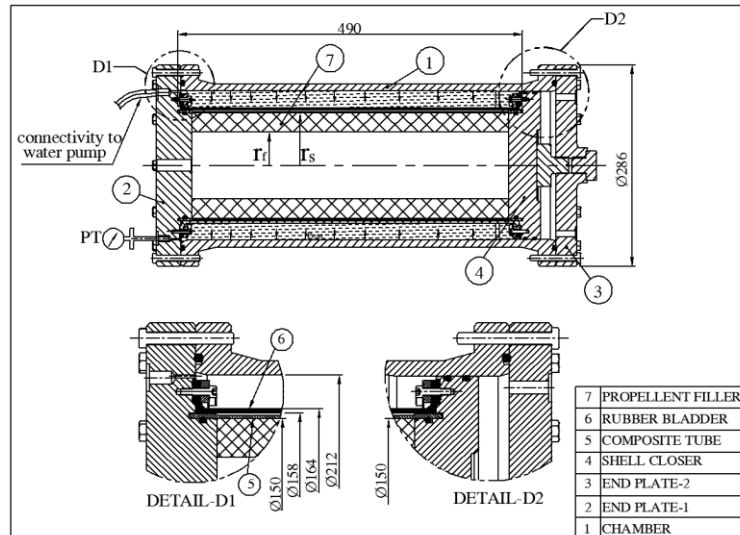


Figure 7: Schematic of test setup for external pressure buckling



Figure 8: Stages of assembly of hardware for testing

The setup has a provision to fill water and pressurize the annular gap between the shell and the pressure chamber using pneumatic driven pump to apply external pressure to the specimen tube. Two pressure transducers are connected to the pressure chamber to record time history of pressurization. A suitable computerized data acquisition system is used to acquire the pressure data at the rate of 100 samples per second. Typical pressure time history record of the annular volume between the chamber and the tube is presented in Figure 9. The first pressure peak in the curve, after which annular pressure drops, is considered as the initiation of buckling of the composite tube. This pressure is referred to as experimental critical pressure,  $P_{cr}$ . Once the shell starts to buckle, the annular volume increases and the pressure starts dropping after this point.

#### 4. Finite Element Analysis

Finite element (FE) analysis was done in this study to predict the behavior of empty and filled tubes. The composite shell was modeled using shell-181 while the solid elastic propellant was modeled using solid-186 element of commercially available ANSYS software.

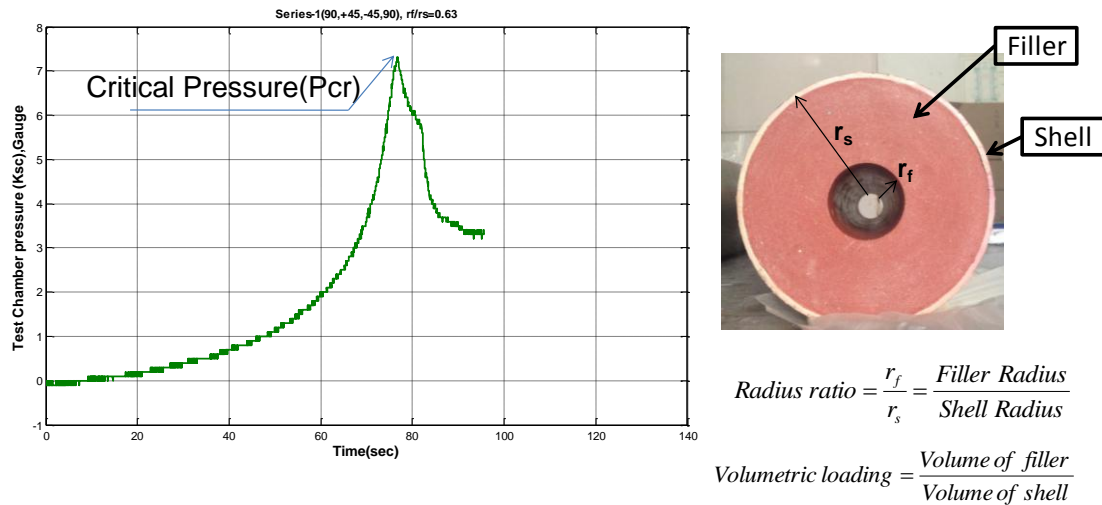


Figure 9: Typical time history of pressure indicating the critical pressure

Solid-186 is a 3-D 20-noded solid element with six degrees of freedom at each node whereas shell-181 is a 4-noded element with six degrees of freedom at each node. Shell element caters for modeling the filament wound structure as a layered element. The shell elements available for modeling layered composites in ANSYS are shell-181 and shell-281, and both of them are suitable for analyzing thin to moderately-thick shell structures. Both are Reissner-Mindlin shell theory elements and are well suited for large strain nonlinear applications. Nevertheless, an advantage of shell-181 over shell-281 is the reduced computation time required for solving the problem.

The accuracy of results by shell-181 to a particular problem is checked by mesh refinement studies. In this case, four layers of 0.5mm each with appropriate layer property were defined in shell element of the FE model. Figure 10 shows typical mesh adopted for the structure. Mesh convergence studies were taken up to select the size of elements. Convergence is taken with respect to the size of elements in terms of the curvature normal angle ( $\Phi$ ) and linear size (h) as indicated in Figure 11. Based on the results of this study,  $\Phi = 3^\circ$  and h = 4mm is selected for all FE modeling.

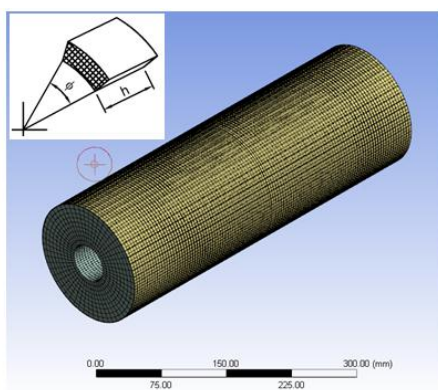


Figure 10: Typical mesh adopted for FE modeling

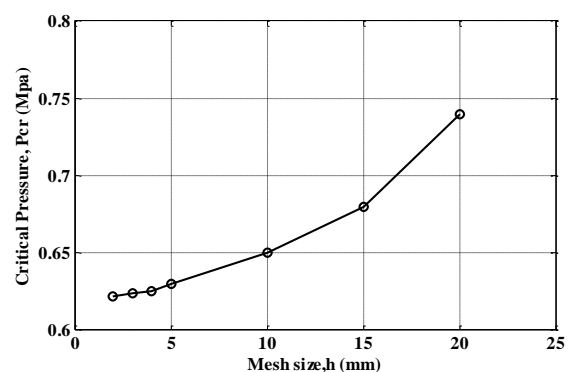


Figure 11: Mesh size convergence study results

The physical element size of 4mm x 4mm is reasonably good for the modeling. Clamped boundary condition was applied to either ends of the shell but the filler ends were not constrained. The external pressure was applied in steps to complete the non-linear analysis. At every step of the load application, deformed geometry of the tube due to previous load step was updated. Initial geometric imperfection of magnitude 0.1mm in the radius was considered for the non-linear buckling analysis. Using uni-axial test

data reported in previous Figure 5, two-parameter Mooney-Rivlin model was extracted and used to represent the engineering property of the elastic filler propellant. Convergence of the solution was monitored to ensure convenience of each load stop. Pressure load versus radial displacement history of the tube structure was extracted from the FE analysis. Typical convergence graph reported in ANSYS is presented in Figure 12. The instability instance is indicated as the bisection occurrence point, which is the instance marked as the critical load.

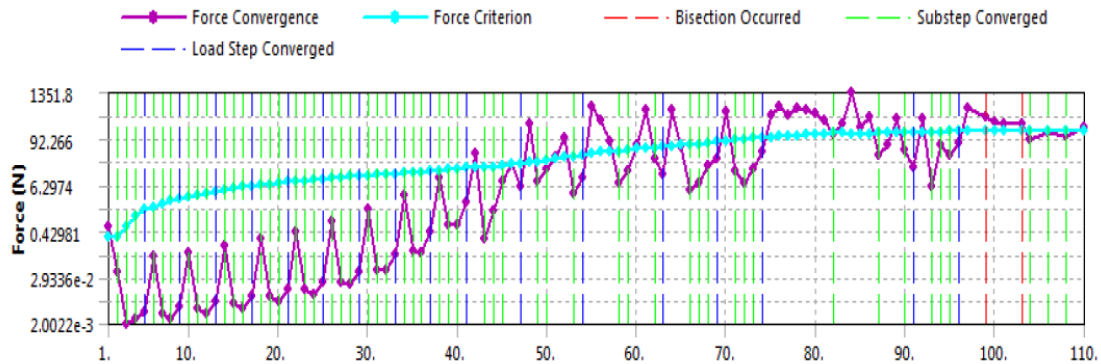


Figure 12: Convergence plot in ANSYS

Plots of load-displacement curves and critical pressure for Series-1 and Series-2 glass tubes are as presented in Figure 13 and Figure 14, respectively, for various volumetric loading fractions obtained from FE non-linear analysis. The maximum pressure before initiation of instability is picked up as the Pcr from respective curve. It is observed that there is a small zone of linearity in the load-displacement curves generated in FE simulation. The radial deformation in these linear zones is less than 0.25mm, which is very small in magnitude. On the other hand, nonlinearity is observed early in the response. Since the solution in each load step has converged, the prediction of Pcr is accepted to be accurate. However, the overlapping trend of slope for the curves in the linear zones needs further investigation. In this present study, the focus is to reach the critical pressure zone. Hence 25 load steps were selected for the solution, which is assumed to be adequate.

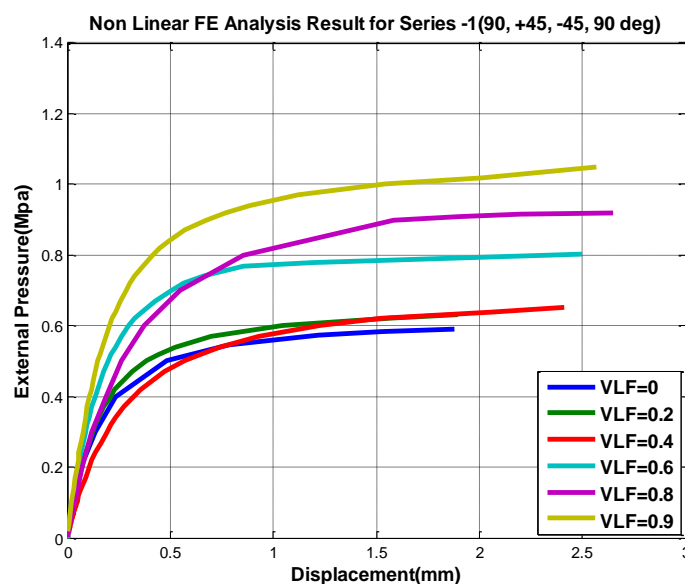


Figure 13: FE based load deflection curve for series-1 tubes



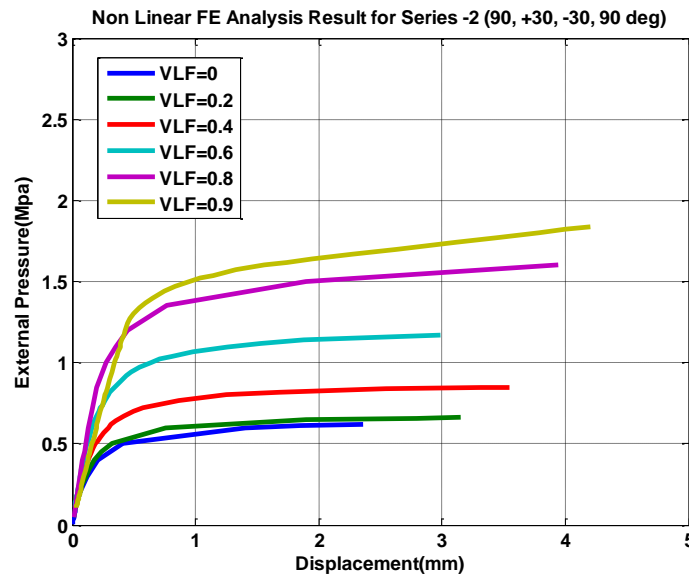


Figure 14: FE based load deflection curve for series-2 tubes

The first mode shapes of the composite tubes that are obtained in the linear buckling analysis with different VLFs are presented in Figure 15. It can be seen that the tubes under external pressure exhibit four full lobes circumferentially and one half lobe in longitudinal direction. No mode shape pattern change is observed between different filling ratios for the given dimensions of the tube combinations and the mechanical properties of tube and elastic filler. Therefore, the increase in VLF is not sensitive in terms of changing the mode shape for the tube under investigation.

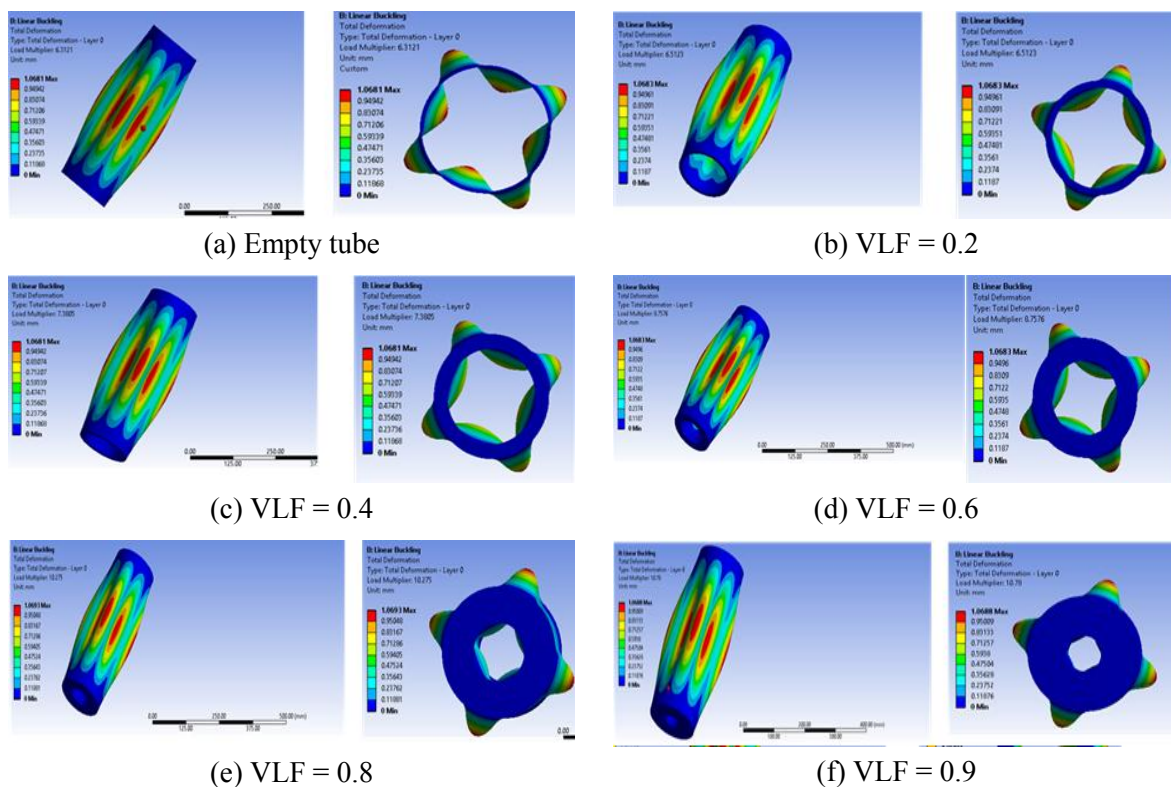


Figure 15: Mode shapes of empty and partially filled tubes under external pressure

**5. Results and Discussion**

Examples of pressure time curves recorded during experiments for Series-1 and Series-2 composite tubes for empty tube and filled tube are presented in Figure 16 and Figure 17. It can be observed that time of rise of the history is different for the three tests due to the manual mode of the presentation. Repetitiveness of test data for the same volumetric loading can be seen in these two figures as well. Similar test data record was obtained for all volumetric loading fractions for experimental results of both Series-1 and Series-2 tubes. Critical pressure data was extracted from each of these experimental curves. Table 2 and Table 3 summarize the experimental data as recorded in the tests and tabulate the corresponding computed mean of Pcr for Series 1 and Series 2 tubes, respectively. The spread of the experimental data over the mean is also indicated in the tables. Finite element based theoretical critical pressure for Series-1 and Series-2 tubes, derived from previous Figure 13 and Figure 14, are tabulated in Table 2 and Table 3 for comparison.

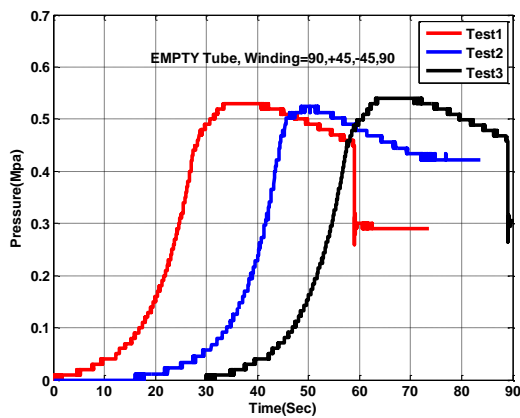


Figure 16: Typical experimental pressure record for Series 1 empty tubes

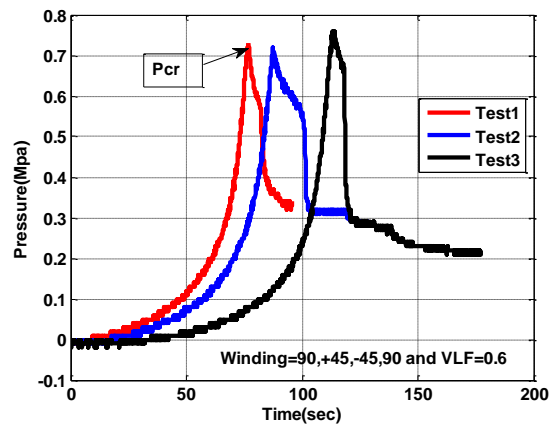


Figure 17: Typical experimental pressure record for Series 1 filled (0.6 VLF) tubes

Table 2: Critical pressure for partially filled tubes of Series-1

Sample No.	Ratio of radius (r <sub>i</sub> /r <sub>s</sub> )	Volumetric loading fraction	Experimental Data			FEM Result (MPa)
			All (MPa)	Mean (MPa)	Spread Over Mean (%)	
1	1.00	0.0	0.540	0.532	+1.5 -0.38	0.590
2			0.530			
3			0.525			
4	0.89	0.2	0.570	0.572	+0.35 -0.35	0.630
5			0.574			
6			0.571			
7	0.77	0.4	0.594	0.595	+0.85 -0.84	0.660
8			0.600			
9			0.590			
10	0.63	0.6	0.730	0.747	+3.1 -2.3	0.800
11			0.740			
12			0.770			
13	0.45	0.8	0.980	1.016	+3.3 -3.7	0.920
14			1.020			
15			1.050			
16	0.31	0.9	1.170	1.155	+1.3 -3.1	1.050
17			1.170			
18			1.120			

Table 3: Critical pressure for partially filled tubes of Series-2

Sample No.	Ratio of radius ( $r/r_s$ )	Volumetric loading fraction	Experimental Data			FEM Result (MPa)
			All (MPa)	Mean (MPa)	Spread Over Mean (%)	
1	1.00	0.0	0.595	0.610	+5.1 -2.5	0.620
2			0.641			
3			0.595			
4	0.89	0.2	0.640	0.673	+6.9 -5.1	0.662
5			0.720			
6			0.660			
7	0.77	0.4	0.880	0.897	+2.5 -1.4	0.849
8			0.920			
9			0.890			
10	0.63	0.6	1.140	1.173	+0.6 -2.9	1.170
11			1.180			
12			1.200			
13	0.45	0.8	1.430	1.477	+4.3 -3.2	1.600
14			1.540			
15			1.460			
16	0.31	0.9	1.950	2.023	+9.7 -3.7	1.840
17			2.220			
18			2.000			

Figure 18 provides the graphical variation of the data spread, which shows a standard deviation of 3.7% over the mean. Comparative analysis graphs of the aforesaid results are presented in Figure 19 and Figure 20 for Series-1 and Series-2 composite tubes, respectively. Results from both experimental and theoretical results using FE analysis highlight the buckling load carrying capacity of the composite tubes has been enhanced up to 1.8 to 3 times as that of an empty tube for a volumetric loading fraction of 0.9. The spread in the experimental data for each set ranges between 2% to 12%, which can be contributed to the variation in cylindricity of the filament wound tubes, resulting in different initial imperfection.

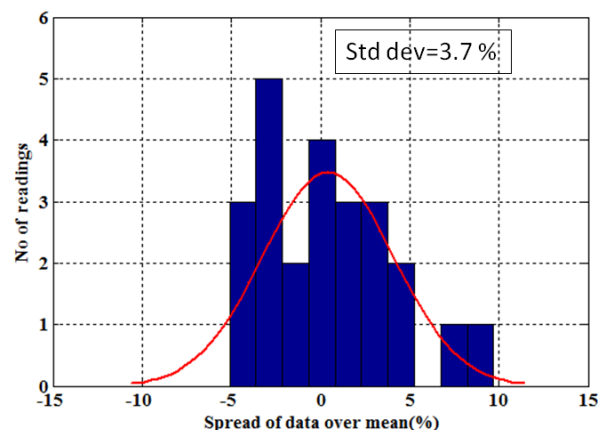


Figure 18: Spread of experimental data obtained for both Series-1 and Series-2 tubes

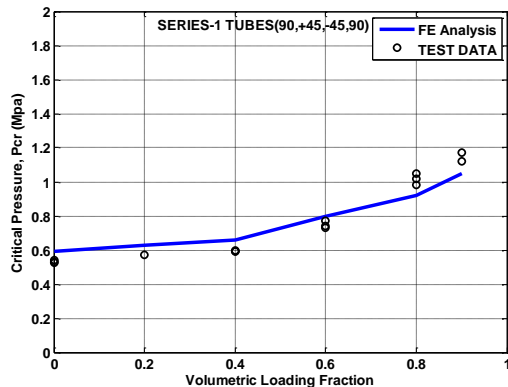


Figure 19: Comparison of experimental data and FE results for Series-1 tubes

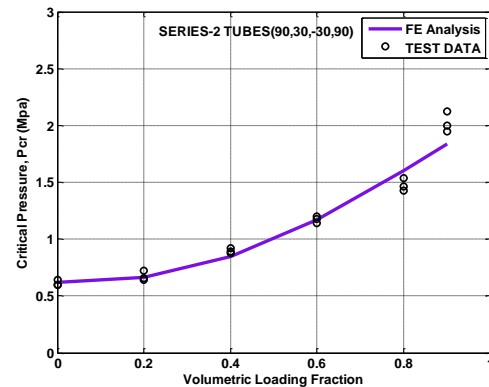


Figure 20: Comparison of experimental data and FE results for Series-2 tubes

## 6. Conclusion

This experimental investigation, which is supported by the theoretical simulation, concludes that there is an improvement in the buckling strength of thin glass composite shells filled with propellants under external pressure. The non-linear FE analysis captures the behavior of the filled tube very closely to the trend established from the experiments (i.e. within 10% accuracy in terms of prediction of Pcr). Volumetric loading fraction of 0.9 with solid propellant equivalent elastic filler increases the strength of the tube in comparison to the empty one by 1.8 to 3 times. This improvement in buckling strength can be utilized for structural optimization of CRMC in rocketry application.

## References

- [1] Seide P 1962 *J AEROSPACE SCI* **29** 851-62
- [2] Seide P and Weingarton V I 1962 *American Rocket Society Journal* **32** 680-8
- [3] Kerr A D and Myint T U 1965 *Int J Mech Science* **7** 373-81
- [4] Goree W S and Nash W A 1962 *Experimental Mechanics* **2** 142-9
- [5] Karam N G and Gibson L J 1995 *INT J SOLIDS STRUCT* **32** 1285-306
- [6] Li H P 1998 *Investigation of the stability of metallic/composite cased propellant rocket motors under external pressure* Virginia Polytechnic Institute and State University
- [7] Tsouvalis N G, Ztiraton A A and Paazolou V J 2003 *COMPOS PART B - ENG* **34** 217-26